

Thermal Oxidation of $Ti_{1-x}Al_xN$ Coatings in Air

F. Vaz,^a L. Rebouta,^a M. Andritschky,^a M. F. da Silva^b and J. C. Soares^c

^aUniversidade do Minho, Departamento de Física, 4710 Braga, Portugal

^bITN, Departamento de Física, E.N.10, 2685 Sacavém, Portugal

^cCFNUL, Av. Prof. Gamma Pinto, 2, 1700 Losboa, Portugal

Abstract

(Ti,Al)N coatings prepared by combined DC and RF magnetron sputtering were annealed in air at temperatures between 500 and 900°C, in order to obtain information regarding the oxidation behaviour. The depth concentration profile of the oxidized layers was measured by Rutherford Backscattering Spectrometry (RBS). During the heat treatment at 500°C, the $Ti_{0.35}Al_{0.65}N$ coating forms a Ti and Al mixed oxide with about 10 at% of nitrogen. After the annealing at 600°C of $Ti_{0.62}Al_{0.38}N$ and $Ti_{0.35}Al_{0.65}N$ coatings, the nitrogen amount disappears and the oxide layer is still homogeneous. At temperatures between 750 and 900°C, a two-layer structure is formed, consisting generally in a protective superficial layer of Al_2O_3 with traces of Ti, followed by a titanium-rich zone. The $Ti_{0.35}Al_{0.65}N$ system showed a slightly higher oxidation resistance than the $Ti_{0.62}Al_{0.38}N$ one. On the other hand, the Al-rich coating, $Ti_{0.19}Al_{0.81}N$, revealed the worst oxidation resistance, similar to the AlN coating, and the oxide layer is always homogeneous. © 1997 Elsevier Science Limited.

1 Introduction

Hard nitride coatings are widely used as protective coatings in multiple applications like cutting, punching and moulding tools due to their hardness and good wear resistance. TiN coatings exhibit those properties but have the disadvantage of oxidizing heavily in high temperature applications.^{1,2} One way to improve the performance consists in modifying the coating composition by introducing additives like Al, Cr and C, in some compositions, producing compounds like the now extensively used (Ti,Al)N and Ti(C,N) compounds. These

hard coatings show not only high hardness and low friction coefficient but also good heat, oxidation and corrosion resistance properties. For example, (Ti,Al)N coatings exhibit a great improvement in oxidation resistance when compared with TiN coatings and can be used at temperatures up to 800°C. The oxidation behaviour of these coatings has been investigated by several authors.^{3–11} The $Ti_{0.50}Al_{0.50}N$ coatings form a stable and protective Al_2O_3 layer at the outer surface in an oxidizing environment at temperatures above 700°C. The Al_2O_3 is a highly insulating oxide, with low ion mobility, which limits the oxide growth and acts as an effective oxygen diffusion barrier. This inhibits further oxidation, resulting in a protective oxide film. The objective of the present work is to contribute to the understanding of basic mechanisms in oxide layer formation and on growth kinetics, including the role of the relative Ti and Al content of the coatings.

2 Experimental Details

The (Ti,Al)N coatings were deposited on polished high-speed steel substrates (AISI M2) by reactive magnetron sputtering. Prior to deposition, the substrates were in-situ r.f. sputter etched in argon (200 W during 15 min). Afterwards, depositions were carried out in an atmosphere of argon and nitrogen at a total pressure of about 0.4 Pa, using Ti and Al pure targets in an Alcatel SCM 650 system. The nitrogen flow rate was adjusted to values from 4 to 5.25 cm³ min⁻¹ and the Argon flow rate was always 100 cm³ min⁻¹. The target to substrate distance was kept constant at 60 mm. The typical base pressure in the deposition chamber was about 1 × 10⁻⁴ Pa. The substrates were heated to 300°C and rotated with a frequency of 10 rpm over the targets. The Ti target was coupled to a RF source

(13.51 MHz), while the Al target was DC, biased and a negative DC bias of -50 V was applied to the substrates during all runs. In order to study the oxidation behaviour, the samples were annealed in air at temperatures between 500 and 900°C after coating deposition.

The morphology of the coatings and the films thickness were studied by Scanning Electron Microscopy (SEM). The structure of the (Ti,Al)N coatings was determined by X-ray diffraction analysis. The X-ray diffractometry system, Philips PW1710, was operated with $\text{CuK}\alpha$ radiation and the analyses were performed in a powder diffraction mode (40 kV, 30 mA, irradiated length of 12 mm). Rutherford Backscattering Spectrometry (RBS) was used to study the composition and the depth concentration profiles. During the RBS experiments, a 2.0 MeV He^+ beam was directed onto the sample surface and a surface layer with a thickness up to $0.2\ \mu\text{m}$ was analyzed. For information about deeper layers, the nitrogen and the oxygen content of the nitrides were obtained using a 1.7 MeV H^+ beam. The backscattered particles were detected by two surface barrier detectors placed at a 140° and 180° to the beam direction. The samples with relatively thin oxidized surface layers were tilted 70° relative to the analyzing beam direction to improve the depth resolution. The RBS spectra were fitted with the RUMP code.¹² The surfaces of some samples were also analysed by X-ray photoelectron spectroscopy (XPS), which was performed using the $\text{Mg K}\alpha$ radiation as excitation source. The binding energy for the atomic levels was corrected for the value of carbon contamination C 1s at 284.6 eV.

3 Results and Discussion

3.1 Characterization of the 'as deposited' coatings

The composition of the studied samples determined by RBS technique is presented in Table 1. The nitrogen atomic composition of the studied samples is about 50 at%, within an error of about 3 at%. This implies that there is also the same error in the total amount of Ti + Al, but not in the Al/Ti concentration ratio of which the accuracy was about 0.01 . Oxygen was not detectable by RBS in the as-deposited samples, even using a proton beam, which means that the oxygen content of the

as-deposited samples is less than 2 at%. X-ray diffraction analyses show for $\text{Ti}_{0.62}\text{Al}_{0.38}\text{N}$ and $\text{Ti}_{0.35}\text{Al}_{0.65}\text{N}$ samples a strong (111) texture indexed with the cubic B1 NaCl structure typical for TiN. For $\text{Ti}_{0.35}\text{Al}_{0.65}\text{N}$ diffraction lines of low intensity indexed to the wurtzite structure were also observed, and for $\text{Ti}_{0.19}\text{Al}_{0.81}\text{N}$ a wurtzite structure was found, results which generally agree with literature data.^{11,13}

3.2 Temperature dependence of the oxidation of $\text{Ti}_{1-x}\text{Al}_x\text{N}$ coatings

The composition of the oxide layers formed during the oxidation of (Ti,Al)N samples is strongly dependent on oxidizing temperature and coating composition. The composition of the oxide layer changes with the increase of the annealing temperature. The RBS spectra displayed in Fig. 1, obtained with the as-deposited $\text{Ti}_{0.35}\text{Al}_{0.65}\text{N}$ coating and after annealing in air for 1 h at the indicated temperatures (600 to 900°C), illustrate that behaviour. The measured data are shown as dots and the continuous lines represent the RUMP simulations. From these spectra, the total amount of the oxygen atoms incorporated in the surface coating during each heat treatment (in atoms cm^{-2}) was obtained. This amount is approximately proportional to the area of the oxygen profile in each spectrum.¹⁴ Furthermore, the depth concentration profiles of Ti, Al, N and O can also be obtained. The depth composition profiles of constituent elements of $\text{Ti}_{0.35}\text{Al}_{0.65}\text{N}$ coating oxidized at 500°C during 168 h are represented in Fig. 2(a). After this annealing time, the oxide layer completely covers the surface. The RBS measurement reveals an oxide layer with about 10 at% of nitrogen and an Al to Ti concentration ratio similar to that measured in the as-deposited coating and with an interface oxide/nitride relatively sharp. In the case of the sample oxidized at 600°C (Fig. 2(b)) one can see a homogeneous mixed oxide layer consisting of Ti, Al and O, as already reported for $\text{Ti}_{0.50}\text{Al}_{0.50}\text{N}$ ⁹ and $\text{Ti}_{0.62}\text{Al}_{0.38}\text{N}$.¹⁰ The comparison with the composition of the oxide layer formed at 500°C shows that, at 600°C , the nitrogen disappears from the oxide layer. In Fig. 3, depth composition profiles used for RUMP simulations are shown for the annealing of $\text{Ti}_{0.62}\text{Al}_{0.38}\text{N}$ and $\text{Ti}_{0.35}\text{Al}_{0.65}\text{N}$ coatings at 800°C during 9 h, and of $\text{Ti}_{0.19}\text{Al}_{0.81}\text{N}$ coating at 850°C during 1 h. The thickness scale on the top of the plot is only introduced to indicate a value for the thickness of the oxide layers. Since layers of slightly different densities develop during the oxidation, the thickness scale cannot be accurate. We assumed in all figures a constant average density within the oxide layers, taking into account the Al/Ti ratio of the oxide

Table 1. Composition and thickness of the studied samples

Sample	Ti (at%)	Al (at%)	N (at%)	Thickness (μm)
$\text{Ti}_{0.62}\text{Al}_{0.38}\text{N}$	31	19	50 ± 3	2.9
$\text{Ti}_{0.35}\text{Al}_{0.65}\text{N}$	17.5	32.5	50 ± 3	3.0
$\text{Ti}_{0.19}\text{Al}_{0.81}\text{N}$	9.5	40.5	50 ± 3	5.6

layers. During an annealing at higher temperatures (750 to 900°C), an almost pure outer layer of Al_2O_3 grows on the coating, as reported earlier for $Ti_{0.50}Al_{0.50}N$.³⁻¹⁰ The analysis of the profiles for the samples annealed at 800°C (Figs 3(a) and (b)) shows clearly the enrichment of Al and O in the surface region (ratio 2:3), an intermediate layer consisting essentially in Ti and O and the absence of N in the oxide layer. Nevertheless, it should be noted that even in the outer layer of the oxide layer

growing on the $Ti_{0.35}Al_{0.65}N$ coatings for temperatures between 800 and 900°C, a Ti concentration of about 2at% (4at% in the $Ti_{0.62}Al_{0.38}N$ coating) and in the intermediate layer an Al concentration of about 11at% can be found (2at% in the $Ti_{0.62}Al_{0.38}N$ coating). As regards the depth concentration profiles, it should be mentioned that the half-maximum of the aluminium signal at the interface oxide/nitride lies slightly deeper than that of the O and N signals, as one can see in Figs 3(a)

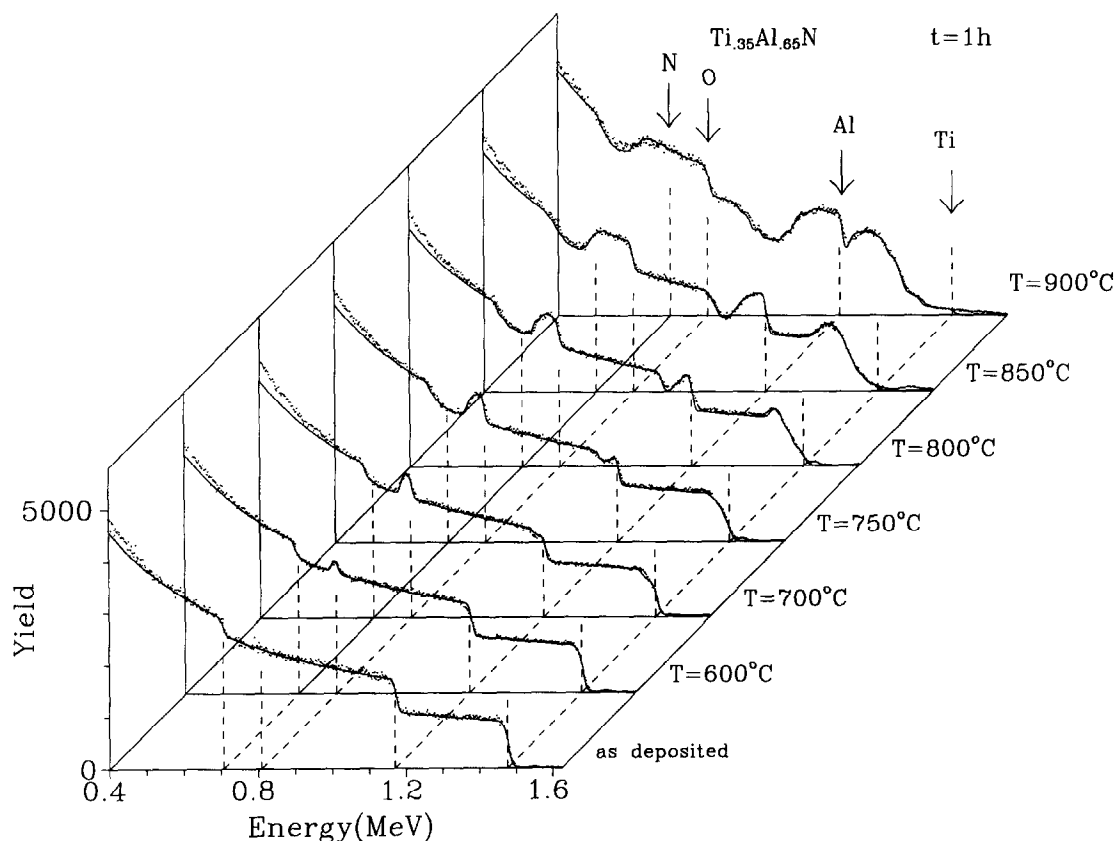


Fig. 1. RBS spectra recorded on as-deposited and after the annealing in air during 1 h at the indicated temperatures of the $Ti_{0.35}Al_{0.65}N$ coating.

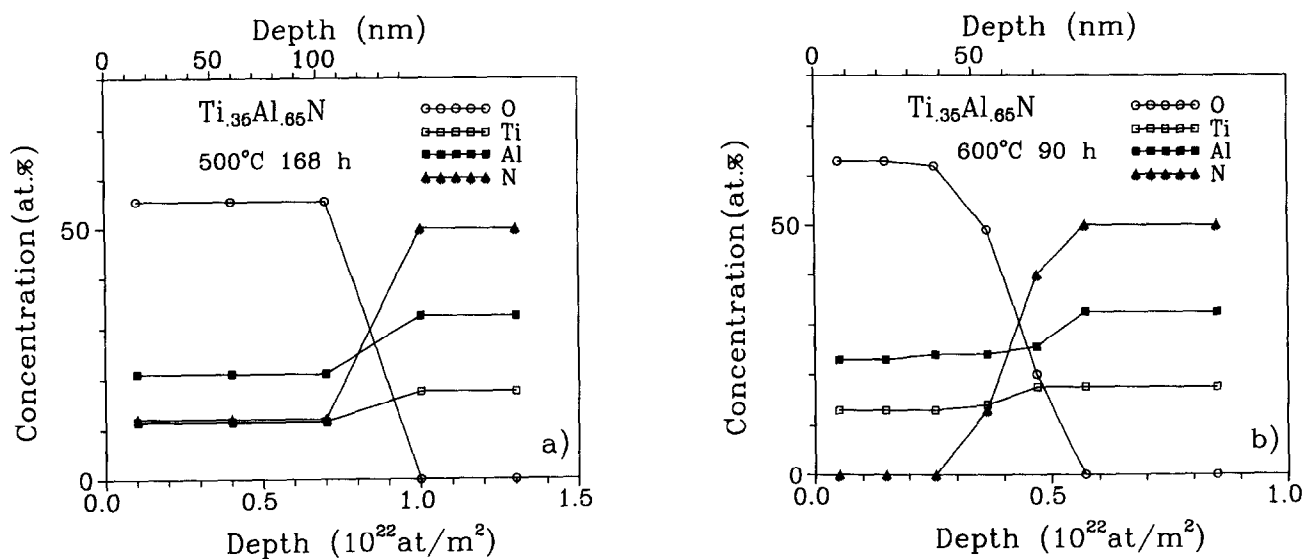


Fig. 2. Depth concentration profiles of Ti, Al, N and O elements of the $Ti_{0.35}Al_{0.65}$ coating oxidized in air at (a) 500°C during 168 h; (b) 600°C during 90 h.

and (b). On the other hand, the Al-rich (Ti,Al)N coating, $Ti_{0.19}Al_{0.81}N$, always forms a homogeneous oxide layer (Fig. 3(c)). The formation of the different oxide layer for the various treatments is summarized in Fig. 4.

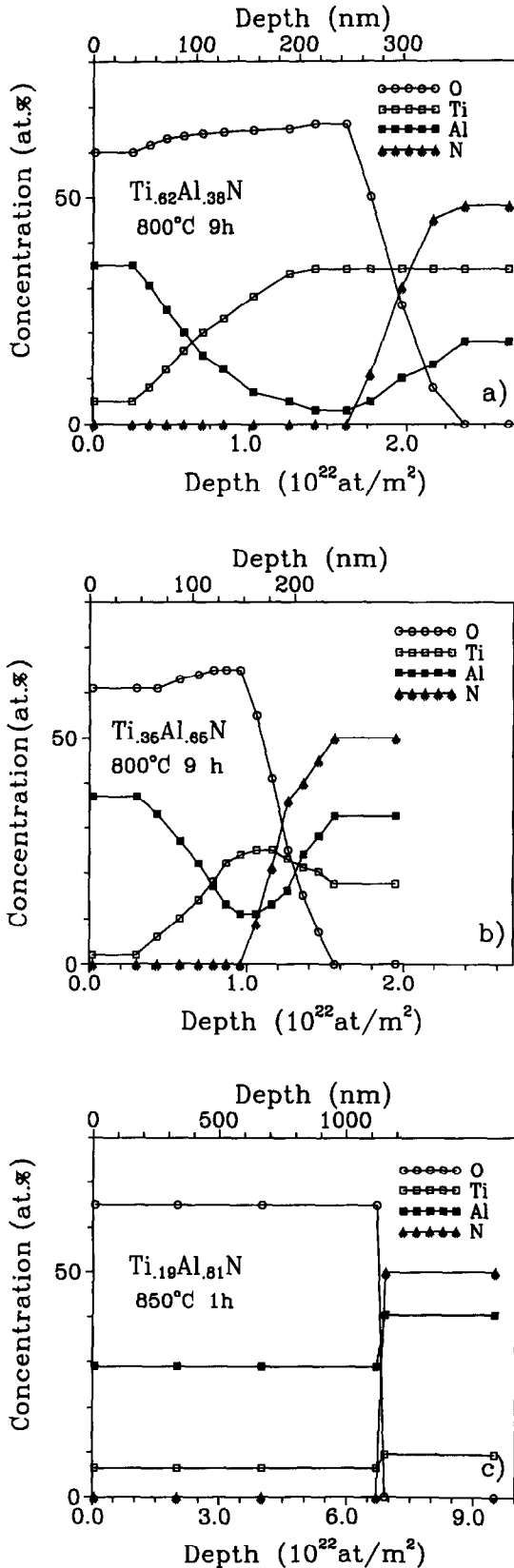


Fig. 3. Concentration profiles of Ti, Al, N and O elements of the following coatings oxidized in air (a) $Ti_{0.62}Al_{0.38}N$ at 800°C during 9 h; (b) $Ti_{0.35}Al_{0.65}N$ at 800°C during 1 h; (c) $Ti_{0.19}Al_{0.81}N$ at 850°C during 1 h.

3.3 Oxidation mechanism

The information gained by the RBS technique is the total amount of oxygen atoms within the oxide layers. The mass of those oxygen atoms for the $Ti_{0.35}Al_{0.65}N$ and $Ti_{0.62}Al_{0.38}N$ coatings is represented in Fig. 5 as a function of the square root of the annealing time for the annealing temperatures of 600 and 800°C. The straight lines fitted to the points represented in the graph show that the growth of oxidation layers for different annealing times ($t=0.5-90$ h) can be described by a parabolic growth law (eqn (1)) with K_p being the parabolic growth rate ($kg^2 m^{-4} s^{-1}$), t , the oxidation time and Δm_{oxygen} the mass of the oxygen atoms in the oxide layer ($kg m^{-2}$) due to the oxidation of the metallic elements:

$$\Delta m_{oxygen}^2 = K_p \cdot t + A \quad (1)$$

where A is a constant, accounting for the 'incubation time'. Based on this assumption, in Fig. 6, the

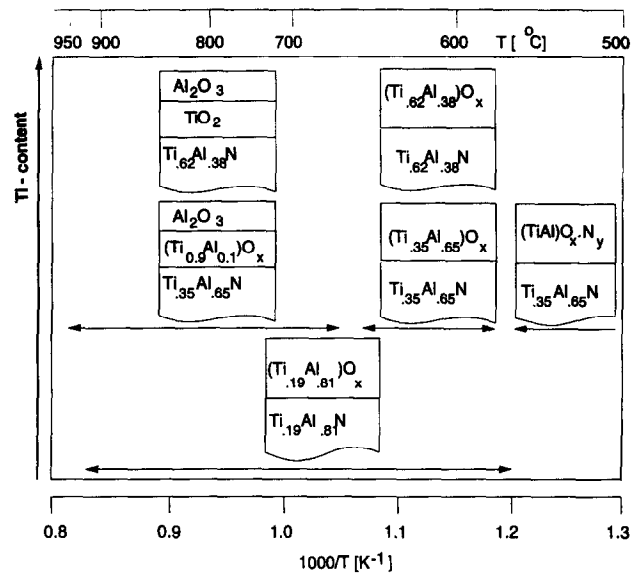


Fig. 4. Schematic diagram of the composition of the different oxide layers formed at the indicated temperatures.

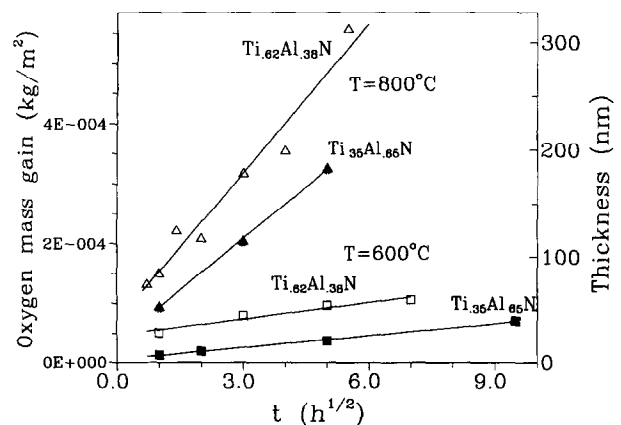


Fig. 5. Mass of incorporated oxygen atoms as a function of the square root of the annealing time.

oxidation rates of our samples are compared with literature data on $Ti_{0.50}Al_{0.50}N^{3,9}$ and AlN^3 coatings. Thus, Fig. 6 represents the mass square of the oxygen atoms incorporated during an annealing time of 1 h, in the form of an Arrhenius plot, as a function of the oxidation temperature. The K values reported in literature data were converted into oxygen mass gain assuming again a parabolic growth rate for an annealing time of 1 h, on the basis of the theoretical density of the participating oxides of 3970 and 4240 kg m^{-3} , for Al_2O_3 and TiO_2 , respectively.¹⁵ The $Ti_{0.35}Al_{0.65}N$ coating shows the best oxidation resistance which is slightly higher than that of $Ti_{0.62}Al_{0.38}N$ and $Ti_{0.50}Al_{0.50}N$ at temperatures between 700 and 850°C , but significantly better at 600 and 900°C . The $Ti_{0.19}Al_{0.81}N$ coating presents the worse oxidation resistance of the studied (Ti,Al)N coatings, which is similar to the oxidation behaviour of AlN . The oxidation resistance increases with the concentration of mol% AlN , at least for values up to $65 \text{ mol}\%$, decreasing again for higher concentrations. This critical concentration coincides with the transition from the NaCl structure to the wurtzite structure. Ikeda *et al.*¹¹ measured the micro-hardness of $Ti_{1-x}Al_xN$ coatings for different values of x and found again a maximum at this critical concentration.

The values represented in Fig. 6 were obtained for an annealing time of 1 h, which means that, for the temperature of 900°C , the thickness of oxide layer for the $Ti_{0.62}Al_{0.38}N$ coating is about three times higher than that formed for the $Ti_{0.35}Al_{0.65}N$ coating. This different thickness of the oxide layer and the Al composition of the Ti rich inner layer can justify the bad performance of $Ti_{0.62}Al_{0.38}N$ coating at this temperature. The increase of the TiO_2 thickness associated with the large difference on the molar volumes of the TiN and TiO_2 , (respectively, 11.4 cm^3 and 18.9 cm^3) results in the

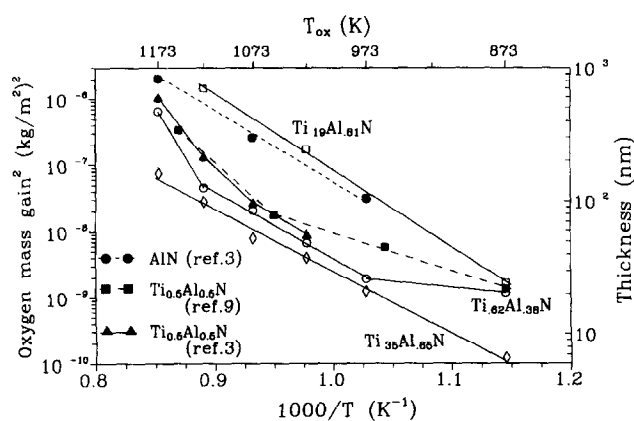


Fig. 6. Mass square of incorporated oxygen atoms as a function of $1/T$ for annealing times of 1 h. The thickness scale on the right side of the graph was only introduced to set a value on the thickness of oxide layers, assuming the same density for all oxide layers.

development of a compressive stress which may lead to a crack formation and the consequent accelerated degradation of the oxidation behaviour. The Al concentration in the Ti-rich inner layer is about $2 \text{ at}\%$ in the case of $Ti_{0.62}Al_{0.38}N$ coating while for $Ti_{0.35}Al_{0.65}N$ coating it is about $11 \text{ at}\%$. The interlayer with the highest Al content grows significantly slower at high temperatures ($T > 900^\circ\text{C}$). We are inclined to attribute the better corrosion resistance of the $Ti_{0.35}Al_{0.65}N$ coatings to the performance of the interlayer rather than to the growing pure Al_2O_3 outer layer.

The slope of the Arrhenius plot indicates the activation energy of the oxidation process. For temperatures between 700 and 850°C , an activation energy of 187 kJ mole^{-1} and 175 kJ mole^{-1} were found, respectively, for $Ti_{0.62}Al_{0.38}N$ and $Ti_{0.35}Al_{0.65}N$, and 197 kJ mole^{-1} for $Ti_{0.19}Al_{0.81}N$ at temperatures between 750 and 850°C . These results are in good agreement with other data on the oxidation of $Ti_{0.50}Al_{0.50}N$ (190 kJ mole^{-1} ⁸ and 212 kJ mole^{-1} ³ in the range 750 – 800°C and 295 kJ mole^{-1} ⁹ observed at temperatures between 780 and 877°C) and AlN (205 kJ mole^{-1} ,¹⁶ in the range 650 – 1100°C , 231 kJ mole^{-1} ¹⁶ between 700 and 900°C , and 255 kJ mole^{-1} ,¹⁷ at temperatures between 900 and 1100°C).

As already described, the oxide layer formed at 500°C is homogeneous with about $10 \text{ at}\%$ of nitrogen, and the one formed at 600°C is still homogeneous but without nitrogen. The RBS technique does not provide any chemical information. Additional X-ray photoelectron spectroscopy studies were made for the $Ti_{0.35}Al_{0.65}N$ coating oxidized at 500°C during 168 h. The XPS spectrum of the as deposited $Ti_{0.35}Al_{0.65}N$ coating shows a main peak at 396.5 eV and a small peak at 399.8 eV , both generally attributed to the N 1s core level. The same coating oxidized at 500°C shows two peaks at 402.6 and 399.4 eV : Nevertheless, the peak at 402.6 eV disappears after the annealing at 600°C . The peak at 396.5 eV can be associated with the existing nitride.^{18,19} Thus, the peak at 402.6 eV can be related to NO_x bonds.¹⁹ Considering these two findings, the attack of oxygen leads to the formation of an oxynitride compound, $(TiAl)_N_xO_y$ at 500°C , which decomposes readily with increasing temperature. However, it should be noted that other authors assigned the 399.8 eV and 402.6 eV peaks to terminally bonded, well and poorly screened $\gamma\text{-N}_2$ states, respectively.¹⁸ According to this interpretation of the XPS spectra, the N atoms could be debonded during the oxidation process and remain in the form of N_2 within the oxide layer. In both cases, at temperatures above 600°C , the nitrogen migrates towards the surface and escape to the gas phase.

In order to understand the thermal stability of the oxide layer formed at different oxidation temperatures, two samples of the $Ti_{0.35}Al_{0.65}N$ coating were oxidized at $600^{\circ}C$ during 90 h and, afterwards, one was annealed in vacuum at $800^{\circ}C$ during 2 h and the other was annealed at the same temperature, but in air during 4 h. In the first case, the oxide formed at $600^{\circ}C$ remained stable, as it should be expected to for the mixed oxide $(Ti,Al)O_2$. $(Ti,Al)O_2$ is generally stable up to $1000^{\circ}C$ in vacuum.²⁰ During the $800^{\circ}C$ annealing in air, an Al-rich superficial layer was formed, but with a Ti concentration slightly higher than that of the sample oxidized at $800^{\circ}C$ in air, in contrast to the findings during the vacuum annealing. In air, Al migrates to the surface and forms Al_2O_3 , although with some traces of Ti. The oxidation behaviour during the thermal annealing in air is consistent with that suggested by some authors^{3,7-9} where these duplex scales are a characteristic of oxidation where Ti oxidizes preferentially. This leads to the occurrence of a two-way diffusion process with the outer oxide being formed as a result of the Al diffusion and the inner layer by the simultaneous inward transport of oxygen to the nitride/oxide interface.

4 Conclusions

The thermal oxidation of $Ti_{1-x}Al_xN$ in air was studied. During the annealing of $Ti_{0.35}Al_{0.65}N$ at $500^{\circ}C$ an homogeneous oxide mixture grows with about 10 at% of nitrogen and about 55 at% of oxygen. Oxidation at $600^{\circ}C$ leads to an oxide without nitrogen, consisting in a Ti/Al ratio according to the ratio in the deposited nitride, except for $Ti_{0.62}Al_{0.38}N$ coating and long annealing times, whose oxide layer showed a slight Al enrichment. At temperatures from 750 to $900^{\circ}C$, $Ti_{0.62}Al_{0.38}N$ and $Ti_{0.35}Al_{0.65}N$ form an Al-rich surface layer followed by an Al-depleted inner layer during oxidation. The oxidation rate is controlled by the Al_2O_3 layer growth on the surface and the growing intermediate $(Ti,Al)O_x$ layer, as can be seen from the comparison of our oxidation data with data for pure AlN coatings. The oxidation resistance increases with the concentration of AlN mol%, at least for values up to 65 mol%. For higher Al/Ti ratios, the oxidation resistance of $(Ti,Al)N$ is somewhat reduced and becomes comparable to that of pure AlN. This critical concentration coincides with the transition from the NaCl structure to the wurtzite structure.

The absence of the Al_2O_3 protective layer leads to an oxidation resistance at $600^{\circ}C$ similar to that obtained at $700^{\circ}C$ for the $Ti_{0.62}Al_{0.38}N$ coating.

The increase of Al concentration in the $Ti_{0.35}Al_{0.65}N$ coating decreases the oxygen diffusion rate through the mixed oxide, thus increasing the oxidation resistance at $600^{\circ}C$.

Acknowledgements

The authors gratefully acknowledge the financial support of the 'Junta Nacional de Investigação Científica' (JNICT) during the course of this research under project PBICT/P/CTM/1962/95. We also thank Dr Carlos Sá at CEMUP for help in performing XPS spectra.

References

1. Wittmer, M., Noser, J. and Melchior, H., Oxidation kinetics of TiN thin films. *J. Appl. Phys.*, 1981, **52**, 6659-6664.
2. Suni, F., Sigurd, D., Ho, K. T. and Nicolet, M. A., *J. Electrochem. Soc.*, 1983, **130**, 121.
3. McIntyre, D., Greene, J. E., Hakansson, G., Sundgren, J. E. and Munz, W. D., Oxidation of metastable single-phase polycrystalline $Ti_{0.5}Al_{0.5}N$ films: kinetics and mechanisms. *J. Appl. Phys.*, 1990, **67**, 1542-1553.
4. Knotek, O., Münz, W. D. and Leyendecker, T., Industrial deposition of binary, ternary and quaternary nitrides of titanium, zirconium and aluminum. *J. Vac. Sci. Technol.*, 1987, **A5**, 2173-2179.
5. Hofmann, S. and Jehn, H. A., Selective oxidation and chemical state of Al and Ti in $(Ti,Al)N$ coatings. *Surf. Interf. Anal.*, 1988, **12**, 329-333.
6. Münz, W., *J. Vac. Sci. Technol.*, **A4**, 2717-2725.
7. Jehn, H. A., Hofmann, S. and W. D., Surface and interface characterization of heat treated (Ti,Al) coating on high speed steel substrates. *Thin Solid Films*, 1987, **153**, 45-53.
8. Hofmann, S., Formation and diffusion properties of oxide films on metals and on nitride coatings studied with Auger electron spectroscopy and X-ray photoelectron spectroscopy. *Thin Solid Films*, 1990, **193/194**, 648-664.
9. Joshi, A. and Hu, H. S., Oxidation behaviour of titanium-aluminium nitrides. *Surf. Coat. Technol.*, 1995, **76-77**, 499-507.
10. Rebouta, L., Vaz, F., Andritschky, M. and da Silva, M. F., Oxidation resistance of $(Ti,Al,Zr,Si)N$ coatings in air. *Surf. Coat. Technol.*, 1995, **76-77**, 70-74.
11. Ikeda, T. and Satoh, H., Phase formation and characterization of hard coatings in the Ti-Al-N system prepared by the cathodic arc ion plating method. *Thin Solid Films*, 1991, **195**, 99-110.
12. Doolittle, L. R., Algorithms for the rapid simulation of Rutherford backscattering spectra. *Nucl. Inst. and Meth.*, 1985, **B9**, 344-351.
13. Tanaka, Y., Gur, T. M., Kelly, M., Hagstrom, S. B. and Ikeda, T., Structure and properties of $(Ti_{1-x}Al_x)N$ films prepared by reactive sputtering. *Thin Solid Films*, 1993, **228**, 238-241.
14. Chu, W. K., Mayer, J. W. and Nicolet, M. A., *Rutherford Backscattering Spectroscopy*. Academic Press, New York, 1978, p. 108.
15. Samsonov, G., *The Oxide Handbook*, IFI/Plenum, New York, 1982, p. 19.
16. Guiochon, G. and Jacqué, L., *Bull. Soc. Chim.*, 1963, **836**.

17. Lavrenko, V. A. and Alexeev, A. F., *Ceram. Int.*, 1983, **9**, 80.
18. Saha, N. C. and Tompkins, H. G., Titanium nitride oxidation chemistry: an x-ray photoelectron spectroscopy study. *J. Appl. Phys.*, 1992, **72**, 3072-3079.
19. Wu, H. Z., Chou, T. C., Mishra, A., Anderson, D. R., Lampert, J. K. and Gujrathi, S. C., Characterization of titanium nitride thin films. *Thin Solid Films*, 1990, **191**, 55-67.
20. Luthier, R. and Lévy, F., Magnetron sputtered TiAlON composite thin films I: structure and morphology. *J. Vac. Sci. Technol.*, 1991, **A9**, 102-109.